Proceedings of the 28th IEEE
EMBS Annual International Conference
New York City, USA, Aug 30-Sept 3, 2006

Integrative Analysis of Intracranial Pressure and R-R Interval Signals: a Study of ICP B-Wave using Causal Coherence

Xiao Hu, *Member IEEE*, Valeriy Nenov, and Marvin Bergsneider

Abstract— **Causal coherence analysis was applied to beat-to-beat mean Intracranial pressure (ICP) and RR interval signals that were recorded from twelve normal pressure hydrocephalus patients. Data were organized into two groups including an ICP B-Wave group and a control baseline group. Maximal classic coherence between ICP and RR interval within [0.04 0.15] Hz was found to be significantly greater than zero for both B-wave and control groups. Causal coherence analysis further revealed that feedforward coherence due to RR interval's effect on ICP always exists for both B-wave and baseline ICP state while feedback coherence from ICP to RR interval was enhanced during the occurrence of B-wave.**

I. INTRODUCTION

Intracranial pressure (ICP) is an important physiological signal for the diagnosis and management of patients of various neurosurgical and neurological diseases including brain injury, stroke and hydrocephalus. ICP is the intracranial response to cardiovascular volumetric load and thus contains information for characterizing the dynamics of the tightly coupled cerebrospinal fluid (CSF) and cerebral blood flow (CBF) circulatory systems in both normal and diseased states. Despite the great potential of using ICP to study the above physiological systems, the most popular ICP measure used by clinicians is still its mean value over certain period of time. Hence, subtle but critical information is often lost due to this simple processing of ICP signal. Encouragingly, computerized processing of ICP has become increasingly popular and sophisticated as evidenced by several recent publications [1], [2] that introduced novel methods for ICP signal processing. These recent efforts demonstrated that much information could be extracted by an integrative analysis of ICP with other related signals including arterial blood pressure (ABP) and cerebral blood flow velocity (CBFV). The present work aims to characterize the interdependency between ICP and hear rate variability (HRV) signals using a recently introduced method of causal spectral analysis [3].

Causal spectral analysis was originally introduced for processing RR interval and beat-to-beat systemic blood pressure. Traditional spectral analysis methods can only compute the linear coherence between two signals as a function of frequency while the causal approach is additionally able to differentiate between the direction of coupling. Even though this approach assumes a linear time-invariant dynamic system for signal generation, it has been demonstrated to be effective in characterizing the complex interactions among HRV, ABP and respiratory signals [4] and in characterizing the Baroreflex effect [3]. ICP's spectral contents are similar to those of ABP, therefore, the causal spectral analysis is expected to be applicable for analyzing RR interval and beat-to-beat ICP changes.

As a non-intrusive condition for studying the cardio-cerebral interaction, episodes of ICP B-wave provide ideal materials for testing the above method. ICP B-wave was first described by Lundberg in 1960s [5] as a rhythmic spontaneous oscillation of ICP with a duration of 0.5-2 minutes. Oscillations with similar frequencies to ICP B-wave have been observed in other physiological signals, both intracranial and extracranial ones. Cerebral blood flow velocity (CBFV) through large cerebral arteries has demonstrated B-wave-like oscillations [6]. Local CBFV at small cerebral arteries, measured using Laser Doppler, also has provided evidence for the existence of similar oscillatory activity [7]. Animal studies have directly established the existence of oscillations of pial arterial diameters of cats that were synchronized with ICP B-wave [8]. These demonstrations of B-wave-like patterns in cerebral hemodynamic variables including CBFV and vessel diameters support the concept that ICP B-wave is related to cerebral vascular dynamics. Given these cardio and cerebral vascular relevances of ICP-wave, application of the integrative analysis of ICP and RR interval signals to B-wave episodes is thus particulary appropriate in validating the effectiveness of the methods on one hand and in discovering useful information regarding the interaction of ICP and RR interval variations on the other hand.

II. METHODS

A. Bivariate Autoregressive Model and Spectral Analysis

Causal spectral analysis starts with the classic parametric cross-spectral analysis. A bivariate autoregressive model (AR) is used to model a vector time series ($\mathbf{x}_n$) such that

$$\mathbf{x}_n = \sum_{k=0}^{p} A(k)\mathbf{x}_{n-k} + \mathbf{w}_n \tag{1}$$

where $A(k) = \begin{bmatrix} A_{11}(k) & A_{12}(k) \\ A_{21}(k) & A_{22}(k) \end{bmatrix}$ is AR coefficient matrix, p is the model order. $\mathbf{w}_n$ represents a white noise series and is uncorrelated with $\mathbf{x}$.

Given this model structure, the transfer matrix $H(f)$ in the frequency domain (f) can be calculated as

$$H(f) = (I - A(f))^{-1} \tag{2}$$

where I is the identity matrix and

$$A(f) = \sum_{k=0}^{p} A(k)e^{-j2\pi fk} \tag{3}$$

Xiao Hu,Valeriy Nenov, and Marvin Bergsneider are with the Division of Neurosurgery,University of California, Los Angeles.

1-4244-0033-3/06/$20.00 ©2006 IEEE.

Then the power spectral density matrix $P(f)$ is obtained as

$$P(f) = \begin{bmatrix} P_{11}(f) & P_{12}(f) \\ P_{21}(f) & P_{22}(f) \end{bmatrix} \quad (4)$$

$$= H^*(f)\Sigma H^T(f) \quad (5)$$

where Σ is the covariance matrix of white noise $\mathbf{w}_n$

The classic coherence $\mathrm{CC}(f)$ is then calculated as

$$CC(f) = \frac{|P_{12}(f)|}{\sqrt{P_{11}(f)P_{22}(f)}} \quad (6)$$

Denote nth sample of ICP signal as icp_n and nth sample of RR interval as rr_n, $\mathbf{x}_n$ is arranged as $\begin{bmatrix} rr_n \\ icp_n \end{bmatrix}$ in the present work. Therefore, the causal coherence when RR interval change drives ICP without any feedback from ICP can be obtained as

$$CC_{rr\to icp}(f) = CC(f)|_{A_{12}(i)=0,\, i=0,\ldots,p} \quad (7)$$

Similarly, causal coherence when ICP drives RR interval change can be obtained as

$$CC_{icp\to rr}(f) = CC(f)|_{A_{21}(i)=0,\, i=0,\ldots,p} \quad (8)$$

It should be noted that $A(0)$ has a priori structure such that there is only one non-zero term in $A(0)$ and that it should be located at off-diagonal position [9]. As observed clinically, a prolonged RR interval would decrease diastolic ICP and hence mean ICP within the same RR interval. Therefore, the non-zero term is allocated to $A_{12}(0)$.

B. Model Order Selection

The combined information criterion (*CIC*) for vector AR model as proposed in [10] was adopted in the present work for model order selection. *CIC* was shown to be an optimal criterion in terms of balancing the penalty of model underfit and that of model overfit. *CIC* was calculated according to

$$CIC(k) = Nlog(RES(k)) + Nm\left(\prod_{i=1}^{k}\frac{1+mv_i}{1-mv_i}\right) \quad (9)$$

where $RES(k)$ is the determinant of the estimate covariance matrix of the residual vector of a k-th order AR model, m is the dimension of vector time series and N is the total number of samples in fitting the model. v_i is the finite sample variance coefficient and was given as

$$v_i = \frac{1}{N - im + 1} \quad (10)$$

Based on *CIC*, the optimal order is determined as the k where $CIC(k)$ is the minimum.

C. Detection of Zero Coherence

Based on the previous work [11], surrogate data was preferred for generating the zero coherence function for each data instance. Specifically, two univariate AR models were fitted to RR interval and beat-to-beat mean ICP series, respectively. Then multiple surrogate pairs were generated by simulating the resultant univariate AR models with different realizations of Gaussian white noise series whose variances were determined from the model fitting process. In the present work, 30 surrogate pairs were generated for each data instance and subjected to the same causal coherence analysis. The zero coherence threshold was set to the average surrogate coherence plus two times of its standard deviation.

D. Data Acquisition and Processing

Twelve patients who underwent pre-operative workup for diagnosing normal pressure hydrocephalus (NPH) showed prominent B-wave episodes in their overnight recordings. Simultaneous ICP and ECG were acquired by using a dedicated data acquisition mobile cart loaded with a PowerLab^{TM} acquisition system that interfaced with the Codman ICP Express Box and the GE bedside cardiovascular monitors. Signals were sampled at 400 Hz for a proper heart beat delineation. The insertion of ICP sensor and data acquisition were conducted with proper IRB approval and written consent from patients. Data were recorded as soon as possible after setting up the Codman ICP express box and lasted for twelve hours until the morning on the second day after admission.

Overnight recordings were reviewed using the program Chart 5.0 to locate the episodes of prominent B-wave (amplitude > 5 mmHg). One five-minute segment with B-wave and one five-minute baseline segment that either preceded or followed the selected B-wave segment were then exported for further processing. Consequently, the extracted segments were organized into two groups. The first group contains all segments with ICP B-wave and the second group contains their corresponding baseline segments.

An automatic ICP latency analysis program [12] was used for an easy extraction of RR interval and beat-to-beat mean ICP series. This latency analysis program has a built-in safeguard for both missed and spuriously detected ECG beats. The resultant RR interval series were further visually inspected for any remaining outliers that were due to the misbehavior of beat detection. The resultant beat-to-beat series were then re-sampled at 2 Hz using cubic spline.

Classic coherence (CC), feedforward coherence ($\mathrm{CC}_{rr\to icp}$), and feedback coherence ($\mathrm{CC}_{icp\to rr}$) were calculated using the causal spectral analysis. Considering that respiratory modulation could affect both ICP and RR interval, coherence was only evaluated at the low frequency spectrum, ranging from $0.04 - 0.15$ Hz, following the same protocol used in [13]. Specifically, $\mathrm{CC}_{rr\to icp}$ and $\mathrm{CC}_{icp\to rr}$ were evaluated at the frequency where the classic coherence CC is the maximum within the pre-defined low frequency range. Determination of zero coherence was done by submitting all coherence values against the corresponding zero coherence function.

III. Results

Table I lists two important parameters that affect the results of causal coherence analysis. They include the frequency (F_{max}) where classic coherence is maximal within [0.04, 0.15] Hz and the optimal model order (p).

Feedforward causal coherence ($\mathrm{CC}_{rr\to icp}$) and feedback causal coherence ($\mathrm{CC}_{icp\to rr}$) were evaluated at F_{max}. These

TABLE I

LIST OF MAXIMAL COHERENCE FREQUENCY AND OPTIMAL MODEL ORDER FOR EACH CASE.

	F_{max} (Hz)		p	
	B-wave	Baseline	B-wave	Baseline
1	0.12	0.12	10	10
2	0.04	0.04	6	8
3	0.04	0.04	10	10
4	0.04	0.04	10	8
5	0.04	0.04	9	7
6	0.04	0.04	6	8
7	0.04	0.04	6	10
8	0.14	0.14	10	9
9	0.04	0.04	10	10
10	0.06	0.04	8	8
11	0.04	0.14	9	7
12	0.14	0.04	7	8

F_{max}: Frequency at which classic coherence is maximal within [0.04, 0.15] Hz.
p: Optimal model order.

TABLE II

LIST OF COHERENCE VALUES EXTRACTED BY APPLYING THE LINEAR CAUSAL SPECTRAL ANALYSIS TO EACH CASE.

	CC		$CC_{rr\rightarrow icp}$		$CC_{icp\rightarrow rr}$	
	B-wave	Baseline	B-wave	Baseline	B-wave	Baseline
1	0.82	0.94	0.25*	0.48	0.70	0.67
2	0.78	0.57	0.92	0.63	0.30	0.17*
3	0.67	0.26*	0.54	0.13*	0.22	0.16*
4	0.92	0.46	0.91	0.43	0.05*	0.27
5	0.45	0.38	0.25*	0.39	0.39	0.08*
6	0.60	0.39	0.47	0.33	0.46	0.10*
7	0.80	0.66	0.50	0.58	0.43	0.12*
8	0.85	0.66	0.61	0.33*	0.55	0.46
9	0.83	0.73	0.66	0.81	0.32	0.12*
10	0.85	0.78	0.60	0.53	0.35	0.36
11	0.94	0.86	0.66	0.86	0.48	0.07*
12	0.70	0.38	0.51	0.34	0.26	0.08*

'*' is used to denote instances where the calculated coherence value is below the zero-coherence threshold.
CC: Classic coherence.
$CC_{rr\rightarrow icp}$: Feedforward coherence form RR interval to ICP.
$CC_{icp\rightarrow rr}$: Feedback coherence form ICP to RR interval.

values are listed in Table II. Zero coherence as determined by the zero-coherence threshold calculated using thirty surrogates are indicated with $*$. Results shown here clearly indicate that beat-to-beat mean ICP is highly correlated, in the frequency range of [0.04, 0.15] Hz, with RR intervals in both states as evidenced by the non-zero CCs. However, CC of B-wave is significantly larger than that of baseline ($p = 5.2E-4$). Causal coherence analysis further demonstrated that this coherence at baseline was probably due to the feedforward influence of RR interval. In addition, there is no significant difference of this feedforward coherence between B-wave and baseline ($p = 0.10$). Finally, occurrences of B-wave were accompanied with an increased feedback coherence of ICP's influence on RR interval ($p = 0.03$).

Fig. 1 shows an example of B-wave and corresponding baseline ICP and RR signals (case No. 9). Results from causal coherence analysis of these two segments were shown in Fig. 2 where it is clearly demonstrated that $CC_{icp\rightarrow rr}$ was significantly greater than zero for B-wave segment but not

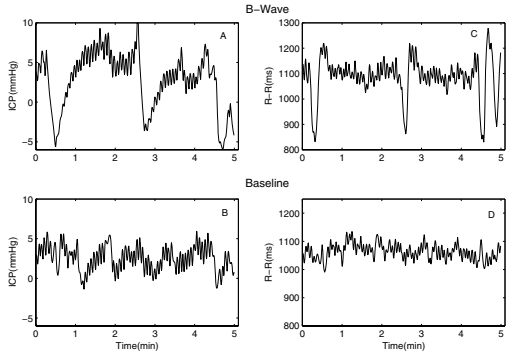

Fig. 1. Representative spline interpolated time series of beat-to-beat mean ICP and RR intervals for both the B-wave and the baseline groups. Data shown were from case No. 9.

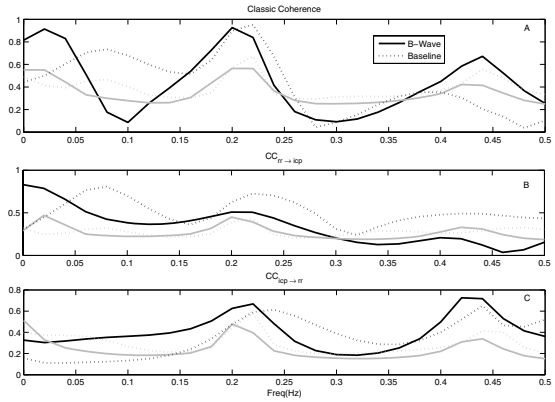

Fig. 2. Classic coherence (CC), feedforward coherence ($CC_{rr\rightarrow icp}$), and feedback coherence ($CC_{icp\rightarrow rr}$) of the case No.9 are shown on panels A, B, and C respectively. Coherence curves for the B-wave group are shown with solid line with their corresponding zero-coherence function curves shown in grey. Dotted line and its grey version are used for showing coherence and zero-coherence curves for the baseline group.

for the corresponding baseline segment.

IV. DISCUSSION

The relationship between beat-to-beat mean ICP and RR interval signals was investigated in the present work. The maximal correlation between them was found to be significant for both the baseline and the B-wave groups within the frequency range of [0.04, 0.15] Hz. This demonstrates a clear vascular origin of the beat-to-beat ICP fluctuations. The causal coherence analysis method revealed additional information regarding the directionality of the coupling between ICP and RR interval, especially the existence of a possible feedback effect from ICP to RR interval. The linear causal spectral analysis showed that this feedback influence of ICP was enhanced during occurrence of B-wave while it was less frequently present for the baseline group (four out of twelve patients showed significantly non-zero $CC_{icp\rightarrow rr}$).

A. Coherence between ICP and RR interval

The feedforward effect from RR interval to ICP is expected as the longer the RR interval is, the smaller the

diastolic value of ICP pulse is. This would then translate into the observed non-zero coherence between the ICP and the RR interval. More interestingly, the causal spectral analysis revealed the existence of a potential feedback effect from ICP to RR interval and that this feedback effect is enhanced during the occurrence of B-wave. This phenomenon, to our knowledge, has not been reported in the existing publications. However, explanation of this feedback effect is not straightforward from the present study. It is possible that this feedback effect is not completely mediated by ICP because changes of beat-to-beat ICP may follow those of systemic arterial blood pressure (ABP). Consequently, the apparent feedback effect from ICP to RR interval could be attributed to that of ABP on RR interval, e.g., the Baroreflex. Additionally, respiratory modulation on ICP and RR interval could be another confounding factor even though we have chosen the frequency of interest below 0.15 Hz.

Even though the lack of ABP measurement in the present work prevents us from drawing a conclusive judgement on whether ICP's feedback effect on RR interval exists, abundant evidence of central organization of cardiovascular rhythms, including RR interval variability, exists in literature that conducted integrative analysis of HRV and other signals other than ICP. This hence suggests a potential role that ICP may play in influencing the control of RR interval variability that originates from central nervous systems. For example, it was reported in [14] that discharge of medullary neurons showed low frequency (LF) rhythmic patterns synchronized with that in HRV while no such LF oscillations existed in simultaneously recorded ABP signals. This suggested that LF HRV oscillations are not necessarily associated with the functional integrity of the baroreceptive mechanism. Furthermore, it is known that in some conditions, e.g., experimental myocardial ischemia LF increase in HRV could occur in the absence of ABP changes [15], [16]. Additional evidence has been obtained from studies involving HRV and direct intraneural microneurograpic recordings of efferent sympathetic nerve traffic to muscle blood vessels (MSNA) and skin blood vessels (SSNA) [17] where synchronous changes in both LF and high frequency (HF) components of both MSNA and RR interval variabilities were found.

B. Methodological issues

As shown in Table I, some variabilities exist in both F_{max} and p even for data cases from same population. Variabilities in F_{max} could be due to inherent uncertainty of determining maximum on a classic coherence curve. It could also be caused by different frequency resolution that was due to different model orders adopted. Different model order could be attributed to inherent variance in model order selection algorithm applied to signals of finite length. Potential effect of these methodological issues on the causal coherence analysis results should be investigated in future studies.

V. Acknowledgements

The present research has been funded by the Brain Injury Research Center (BIRC) with the NINDS funding 441488-MD-19900.

References

[1] X. Hu, V. Nenov, T. C. Glenn, L. A. Steiner, M. Czosnyka, N. Martin, and M. Bergsneider, "Nonlinear analysis of cerebral hemodynamical and intracranial pressure signals: Implication for a nonlinear measure of the autoregulation status," *IEEE Trans Biomed Eng*, vol. 53, no. 2, pp. 195–209, 2006.

[2] R. Hornero, M. Aboy, D. Abasolo, J. McNames, W. Wakeland, and B. Goldstein, "Complex analysis of intracranial hypertension using approximate entropy," *Crit Care Med*, vol. 34, no. 1, pp. 87–95, 2006.

[3] A. Porta, G. Baselli, O. Rimoldi, A. Malliani, and M. Pagani, "Assessing baroreflex gain from spontaneous variability in conscious dogs: role of causality and respiration," *Am J Physiol Heart Circ Physiol*, vol. 279, no. 5, pp. H2558–67, 2000.

[4] L. Faes, A. Porta, R. Cucino, S. Cerutti, R. Antolini, and G. Nollo, "Causal transfer function analysis to describe closed loop interactions between cardiovascular and cardiorespiratory variability signals," *Biol Cybern*, vol. 90, no. 6, pp. 390–9, 2004.

[5] N. Lundberg, H. Troupp, and H. Lorin, "Continuous recording of the ventricular-fluid pressure in patients with severe acute traumatic brain injury. a preliminary report," *J Neurosurg*, vol. 22, no. 6, pp. 581–90., 1965.

[6] R. Zhang, J. H. Zuckerman, and B. D. Levine, "Spontaneous fluctuations in cerebral blood flow: insights from extended-duration recordings in humans," *Am J Physiol Heart Circ Physiol*, vol. 278, no. 6, pp. H1848–55, 2000.

[7] U. Dirnagl, B. Kaplan, M. Jacewicz, and W. Pulsinelli, "Continuous measurement of cerebral cortical blood flow by laser-doppler flowmetry in a rat stroke model," *J Cereb Blood Flow Metab*, vol. 9, no. 5, pp. 589–96, 1989.

[8] L. M. Auer and I. Sayama, "Intracranial pressure oscillations (b-waves) caused by oscillations in cerebrovascular volume," *Acta Neurochir (Wien)*, vol. 68, no. 1-2, pp. 93–100, 1983.

[9] G. Baselli, A. Porta, O. Rimoldi, M. Pagani, and S. Cerutti, "Spectral decomposition in multichannel recordings based on multivariate parametric identification," *IEEE Trans Biomed Eng*, vol. 44, no. 11, pp. 1092–101, 1997.

[10] S. de Waele and P. M. T. Broersen, "Order selection for vector autoregressive models," *Ieee Transactions on Signal Processing*, vol. 51, no. 2, pp. 427–433, 2003.

[11] L. Faes, G. D. Pinna, A. Porta, R. Maestri, and G. Nollo, "Surrogate data analysis for assessing the significance of the coherence function," *Ieee Transactions on Biomedical Engineering*, vol. 51, no. 7, pp. 1156–1166, 2004.

[12] X. Hu, V. Nenov, P. Vespa, and M. Bergsneider, "Automatic analysis of latency of intracranial pressure pulse to r wave of electrocardiogram," *Medical Physics and Engineering*, vol. Submitted, 2006.

[13] L. Faes, L. Widesott, M. Del Greco, R. Antolini, and G. Nollo, "Causal cross-spectral analysis of heart rate and blood pressure variability for describing the impairment of the cardiovascular control in neurally mediated syncope," *IEEE Trans Biomed Eng*, vol. 53, no. 1, pp. 65–73, 2006.

[14] N. Montano, T. Gnecchi-Ruscone, A. Porta, F. Lombardi, A. Malliani, and S. M. Barman, "Presence of vasomotor and respiratory rhythms in the discharge of single medullary neurons involved in the regulation of cardiovascular system," *J Auton Nerv Syst*, vol. 57, no. 1-2, pp. 116–22, 1996.

[15] L. Bernardi, F. Keller, M. Sanders, P. S. Reddy, B. Griffith, F. Meno, and M. R. Pinsky, "Respiratory sinus arrhythmia in the denervated human heart," *J Appl Physiol*, vol. 67, no. 4, pp. 1447–55, 1989.

[16] O. Rimoldi, S. Pierini, A. Ferrari, S. Cerutti, M. Pagani, and A. Malliani, "Analysis of short-term oscillations of r-r and arterial pressure in conscious dogs," *Am J Physiol*, vol. 258, no. 4 Pt 2, pp. H967–76, 1990.

[17] M. Pagani, N. Montano, A. Porta, A. Malliani, F. M. Abboud, C. Birkett, and V. K. Somers, "Relationship between spectral components of cardiovascular variabilities and direct measures of muscle sympathetic nerve activity in humans," *Circulation*, vol. 95, no. 6, pp. 1441–8, 1997.